IEEE Access
Multidisciplinary | Rapid Review | Open Access Journal

Received April 18, 2022, accepted May 5, 2022, date of publication May 12, 2022, date of current version May 19, 2022.

Digital Object Identifier 10.1109/ACCESS.2022.3174690

Predicting Copper and Lead Concentration in Crops Using Reflectance Spectroscopy Associated With Intrinsic Wavelength-Scale Decomposition Spectral Transformation

JIANHONG ZHANG[1], (Student Member, IEEE), MIN WANG[2], KEMING YANG[1], BING WU[1], YAXING LI[1], YANRU LI[1], AND QIANQIAN HAN[1]

[1]College of Geoscience and Surveying Engineering, China University of Mining and Technology-Beijing, Beijing 100083, China
[2]North China University of Science and Technology, Tangshan, Hebei 063210, China

Corresponding author: Keming Yang (ykm69@163.com)

This work was supported in part by the National Natural Science Foundation of China under Grant 41971401, and in part by the Fundamental Research Funds for Central Universities under Grant 2022YJSDC22.

ABSTRACT Hyperspectral remote sensing is a reliable solution for monitoring heavy metal pollution in crops. However, there are few studies on the spectral transformation and estimation of heavy metal content in crops using time-frequency analysis. In this study, intrinsic wavelength-scale decomposition (IWD) was proposed to decompose hyperspectral data to fully exploit the sensitive information implied in them and to investigate the feasibility of the detection of copper (Cu) and lead (Pb) in maize leaves. Leaf spectra and Cu^{2+} and Pb^{2+} contents were obtained from potted maize plants under Cu and Pb stress in the laboratory. After the spectral data were processed using IWD to obtain the proper rotation components (PRC*i*), the characteristic bands were extracted, a Hankel matrix was constructed, and singular value decomposition (SVD) was performed. Finally, singular entropy information was obtained to characterize the heavy metal content. Singular entropy, with a higher correlation with Cu^{2+} and Pb^{2+} contents, was selected to establish the univariate and multivariate partial least squares regression (PLSR) models. The results showed the following: (1) the R^2 of the univariate model for the prediction of copper and lead content was 0.68∼0.81, and the *RMSE* was 0.99∼7.03. (2) The R^2 of the multivariate PLSR model was as high as 0.83, and the *RMSE* was as high as 0.83. This study showed that the characteristic bands can be effectively extracted by IWD spectral transformation, which provides a promising method for estimating heavy metal pollution in vegetation.

INDEX TERMS Crop heavy metal pollution, hyperspectral analysis, intrinsic wavelength-scale decomposition (IWD).

I. INTRODUCTION

In recent years, with industrialization, the discharge of wastewater and waste gas from industrial production has been increasing, resulting in serious soil heavy metal pollution. Heavy metal contamination has serious effects on crop growth and indirectly affects the safety of human diet and health [1], [2]. Heavy metal copper (Cu) and lead (Pb) pollution mainly comes from two aspects: 1) the unreasonable development of mineral resources and the stacking of tailings, and 2) the discharge of wastewater and e-waste in industrial production [3]. Therefore, rapid and accurate monitoring of Cu and Pb contamination in crops has become a global concern for environmental scientists [4]. Cu is an essential trace element for plant growth. Small amounts of Cu in plants are beneficial for plant growth. When the concentration is too high, it will stress the growth of vegetation, inhibit photosynthesis, cause plant metabolism disorders, and even lead to plant death [5]. As a highly dangerous heavy metal, Pb hinders hematopoietic function and affects the cardiovascular, kidney, and nervous systems after being ingested by the human body [6], [7]. Heavy metals are hidden dangers in the

The associate editor coordinating the review of this manuscript and approving it for publication was Yi Zhang.

environment, and comprehensive monitoring of heavy metal pollution is a prerequisite for preventing and controlling environmental pollution and ensuring human health. Monitoring and estimating the degree of Cu and Pb pollution in crops is important [8], [9]. Traditional methods for monitoring heavy-metal pollution mostly focus on field sampling and laboratory chemical analysis, which require considerable time and financial resources and are less efficient [10], [11]. Currently, hyperspectral remote sensing has spectral continuity and high spectral resolution, and has the advantages of low cost, non-destructiveness, and high efficiency for heavy metal pollution monitoring [12], [13]. Healthy plants and those under heavy metal stress exhibit different spectral absorption and reflection characteristics. Hyperspectral remote sensing can rapidly capture the spectral reflectance of plant leaves to realize non-destructive monitoring of heavy metal pollution in plants [14], [15]. These include the detection of mercury (Hg) stress in tobacco leaves [16] and the cadmium (Cd) residue in tomatoes [17].

At present, the commonly used methods for spectral transformation are the first derivative (FD), second derivative (SD), and continuum removal (CR) [18], [19]. Wavelet transform (WT) has powerful analysis capability in the time-frequency domain, and the wavelet transform of spectral data can effectively extract spectral features [20], [21]. Square-root transformation, logarithmic transformation, and reciprocal transformation of spectral data can also highlight the characteristics of spectral reflectance, which is of great significance for improving the prediction of zinc content in the soil [22], [23]. Fractional differential preprocessing of near-infrared spectra can effectively improve the accuracy of model predictions [24]. However, using these methods to extract spectral characteristic parameters not only highlights useful information but also increases noise, which affects the accuracy of heavy metal content prediction to a certain extent. Some researchers have constructed pollution indices using sensitive bands to monitor heavy-metal pollution. Copper stress index (CSVI) and absorption difference vegetation index (ADVI) can detect the degree of crop pollution under copper stress [25]. The chlorophyll index and water stress index had a high correlation with As content in leaves, which could effectively distinguish plant species under heavy metal stress [26]. In addition to this index, some bands can effectively monitor heavy metal pollution. For example, the sensitive bands of rice leaves contaminated by Pb, Zn, Cu, and As are mainly distributed at 460, 560, 660, and 1100 nm, respectively [27]. The bands at 450, 550, 670, 760, and 1240 nm can be used to monitor the concentration of Pb pollution in vegetation [28]. The aforementioned theories are primarily based on conventional methods. Currently, characteristic spectral parameters are commonly used in research worldwide to extract spectral information, such as the sensitive spectral band, spectral vegetation index, and spectral location parameters [29]. These methods have also been studied in the spectral domain. Although the characteristic bands extracted using these methods can effectively improve the prediction of heavy metal concentrations, many factors affect spectral information. To better monitor heavy metal pollution in vegetation, it is necessary to find a more comprehensive spectral information set, improve the reliability of feature information extraction [30], and effectively improve the accuracy of heavy metal content prediction [31].

The hyperspectral monitoring of heavy metal pollution in crops is similar to the detection of abnormal nonlinear signals. Two methods are commonly used in signal anomaly detection: time-domain and frequency-domain analyses. Frequency domain transformation can effectively highlight and amplify abnormal changes in a signal. Some time-domain analysis methods can highlight useful information while retaining the characteristics of the original signal [8], [32]. The spectral responses of crops subjected to heavy-metal stress generally undergo subtle changes. To effectively monitor changes in heavy metal pollution, weak information on the spectral response is enhanced by frequency-domain transformation [33]. Common frequency-domain transform analysis methods include wavelet and Fourier transforms. Time-domain transformation analysis methods include intrinsic time scale decomposition (ITD). ITD is often used for the fault diagnosis of mechanical bearings, heart sound signal processing, etc [34]. However, few researchers have used ITD for hyperspectral data processing and inverting the degree of heavy metal contamination of crops.

Corn is one of the three major food crops in the world and plays an important role in human production and life. Therefore, in this study, corn was taken as the research object, and the common heavy metal Cu and Pb pollution elements were used to predict the heavy metal content of vegetation under Cu and Pb stress. In contrast to previous research, the ITD was improved in this study, and an intrinsic wavelength-scale decomposition (IWD) method was used to estimate the Cu and Pb contents in maize leaves. This study aimed to: (1) obtain hyperspectral data of maize leaves under different concentrations of Cu and Pb stress; (2) extract sensitive bands of maize leaves under Cu and Pb stress by intrinsic wavelength-scale decomposition; and (3) use singular entropy with copper and lead contents to establish univariate and multivariate models for copper and lead content prediction. It has been proven that the inversion model established by IWD has high accuracy and reliability. The method and model proposed in this study can provide a basis for the large-scale monitoring of heavy metal pollution and can also provide a reference for the remediation of heavy metal pollution in mining and agricultural soils. More importantly, we provide new methods and ideas for monitoring heavy metal pollution in soils with a large vegetation cover.

II. MATERIAL AND METHODS

A. EXPERIMENTAL SCHEME

Corns were used as the research object in this study. Potted corn was grown in the laboratory to simulate corn growth under different Cu and Pb concentrations.

The experiments were conducted at the greenhouse laboratory of the China University of Mining and Technology-Beijing in 2017. "Minuo-8" was selected as corn seed. Natural soil samples were collected from the land of Beijing Olympic Park. Debris, plant residues, and other impurities were removed during the soil collection. $CuSO_4 \cdot 5H_2O$ and $Pb(NO_3)_2$ were used as stress reagents. The stress concentrations were designated as 0 μg/g (control group, no stress), 50, 100, 150, 400, 600, 800, and 1000 μg g-1. Three pots of maize were planted for each stress gradient, for a total of 45 maize pots. To facilitate the expression and utilization of the collected maize leaf spectra, the collected average spectra were labeled as shown in Table 1. To maintain the soil water content, water was cultivated three times a day at 7:00 a.m., 12:00 p.m., and 6:00 p.m., 200 ml each time. The air was kept clear and a consistent growth environment was ensured for each potted plant to avoid other factors from affecting the experimental results. A flowchart of the experimental procedure is shown in Figure 1.

TABLE 1. Spectral label of maize leaves.

Stress concentration	Label	
0	CK0 (1)、CK0 (2)、CK0 (3)	
50	Cu50 (1)、Cu50 (2)、Cu50 (3)	Pb50 (1)、Pb50 (2) 、Pb50 (3)
100	Cu100 (1)、Cu100 (2)、Cu100 (3)	Pb100(1)、Pb100(2)、Pb100 (3)
150	Cu150 (1)、Cu150 (2)、Cu150 (3)	Pb150 (1)、Pb150 (2)、Pb150 (3)
400	Cu400 (1)、Cu400 (2)、Cu400 (3)	Pb400 (1)、Pb400 (2)、Pb400 (3)
600	Cu600 (1)、Cu600 (2)、Cu600 (3)	Pb600 (1)、Pb600 (2)、Pb600 (3)
800	Cu800 (1)、Cu800 (2)、Cu800 (3)	Pb800 (1)、Pb800 (1)、Pb800 (1)
1000	Cu1000 (1)、Cu1000 (2)、Cu1000 (1)	Pb1000 (1)、Pb1000 (2)、Pb1000 (3)

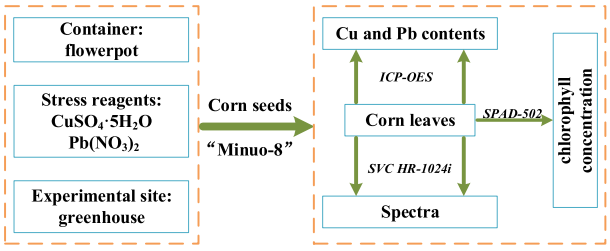

FIGURE 1. The flow chart of the experimental procedure.

B. SPECTRAL DATA ACQUISITION

Spectral data were collected in a dark room, and the spectral data of maize leaves were measured using an SVC HR-1024i spectrometer produced by the Spectra Vista Corporation in the United States. The wavelength range of the SVC HR-1024i spectrometer is 350–2500 nm. A 50 W halogen lamp was used as the light source. The desktop was covered with black cloth to reduce the influence of external stray light and improve the spectral quality. The sensor fiber-optic probe was perpendicular to the blade surface, and the distance was 5 cm, which was the same as when measuring the whiteboard. The field-of-view angle is 25°, ensuring that the projected area of the field-of-view angle falls completely on the leaf surface. Thus, the influence of external stray light can be avoided, and the signals received by the fiber-optic probe are all the spectral information of the leaf sample. To reduce the measurement noise of the reflection spectrum, the spectra of the new, middle, and old leaves were measured thrice, and nine spectral curves were obtained for each potted corn. Finally, the average value of the nine spectral curves was used as the actual spectral data for the leaf sample. When the corn leaf spectrum was collected, the chlorophyll concentration of the leaves was measured separately using a SPAD-502 chlorophyll meter (repeated three times). Finally, the relative values of chlorophyll concentration in corn leaves under Cu and Pb stress were obtained by averaging.

C. CHEMICAL ANALYSIS OF HEAVY METAL CONTENT

Chemical analysis of heavy metal content in corn leaves was performed by the Beijing Academy of Agriculture and Forestry Sciences. After the leaf spectrum data collection was completed, the leaves were washed with deionized water, dried (drying at 70 °C for 48 h), crushed, and the fine particles were sieved and used as leaf samples. Nitric acid and perchloric acid were added for the digestion treatment. Finally, the Cu and Pb contents in the leaves were determined using inductively coupled plasma optical emission spectrometry (ICP-OES) (Thermo Fisher, USA).

D. QUALITY ASSURANCE AND QUALITY CONTROL (QA/QC)

To ensure the authenticity and reliability of the research results, strict quality assurance and quality control (QA/QC) measures were taken during the collection of corn leaves, the measurement of spectral data, and the chemical analysis of heavy metals. The collected corn leaves were cleaned, dried, and stored in special bags. Before measuring the leaf spectral data, a whiteboard was used for calibration to ensure accuracy of the spectral data. Before the detection of heavy metal content, corn leaves were treated in a cleanroom to avoid the interference of pollutants in the surrounding environment. The testing process was quality controlled according to national standard GSB04-1767-2004 to ensure the quality of the analysis.

E. INTRINSIC WAVELENGTH-SCALE DECOMPOSITION (IWD)

Intrinsic wavelength-scale decomposition (IWD) is derived from intrinsic time-scale decomposition (ITD). ITD was first proposed by Mark G. Frei and Ivan Osorio [35]. Compared with empirical mode decomposition (EMD) and wavelet transform, ITD is a new time-frequency analysis method. The

signal component obtained after ITD transformation has relatively complete time-frequency information and can reflect the advantages of signal frequency changes [36]. The purpose of this study was to replace the time (T) in ITD with the wavelength (W), propose and explore the IWD processing technology that forms the spectral signal, and introduce it into the information processing and analysis of hyperspectral data. The IWD can adaptively decompose the wavelength (w) into several proper rotation components (PRC) and trend components (r), and each PRCi component can be obtained by only one iteration. For a spectral curve X_w to be decomposed, an extreme point X_k exists and its baseline extraction operator is defined as L. It can separate the baseline component L_w from the spectral curve X_w to be decomposed, and then define a proper rotation separation operator as H, as in (1).

$$X_w = LX_w + (1 - L)X_w = L_w + H_w \tag{1}$$

where $L_w = LX_w$ is the baseline component, and $H_w = (1 - L)W_w = HX_w$ is the PRC component.

The IWD processing steps of the spectral curve are as follows:

(1) Extract the extreme point X_k on the spectral curve X_w ($k = 1, 2, \ldots, N$; N represents the number of extreme points). τ_k is the set of wavelengths at which the local extreme points of X_w are located. We define $\tau_0 = 0$ as the starting wavelength of X_w and let the values of X_w and L_w at τ_k be X_k and L_k, respectively.

It is assumed that L_w and H_w are defined in the band interval $[\tau_0, \tau_k]$, X_w is defined in the band interval $[\tau_0, \tau_{k+2}]$, and L_w is the affine ray approximation of X_w in the interval $(\tau_k, \tau_{k+1}]$, that is, $L_w = mX_w + n_w$ and $w \in (\tau_k, \tau_{k+1}]$. Because L_w must satisfy the above-mentioned boundary conditions of the local extreme points, *it* is expressed in the following form:

$$L_w = L_k + \frac{L_{k+1} - L_k}{X_{k+1} - X_k}(X_w - X_k) \tag{2}$$

Assuming that the basic trend of the spectral curve is sufficiently smooth, the changes between the local extreme points can be ignored, and it follows that:

$$\frac{X_{k+1} - X_k}{\tau_{k+1} - \tau_k} = \frac{X_{k+2} - X_k}{\tau_{k+2} - \tau_k} \tag{3}$$

Because $L_{k+1} = X_{k+1}$, there are:

$$\begin{aligned} L_{k+1} &= \alpha X_{k+1} + (1 + \alpha)X_{k+1} \\ &= \alpha \left[X_k + \left(\frac{\tau_{k+1} - \tau_k}{\tau_{k+2} - \tau_k} \right) (X_{k+2} - X_k) \right] \\ &\quad + (1 - \alpha) X_{k+1} \end{aligned} \tag{4}$$

where α is a linear scaling factor that can be used to adjust the extracted PRC amplitude ($\alpha \in [0, 1]$) with an empirical value of 0.5.

(2) According to the baseline component derived from Equation (2), calculate and extract the proper rotation component H_w, that is, PRCi;

(3) The baseline component L_w is considered as the input spectrum, and the next decomposition is performed. When the baseline component L_w becomes monotonous or the trend component (r) is smaller than a preset value, decomposition is terminated.

The decomposition process of IWD is shown in formula (5).

$$\begin{aligned} X_w &= H_w + L_w = HX_w + (H + L)LX_w \\ &= \left(H \sum_{k=0}^{p-1} L^k + L^p \right) X_w \\ &= H_w^1 + H_w^2 + H_w^3 + \cdots + H_w^k + L_w^p \end{aligned} \tag{5}$$

where p is the number of PRC, H_w^k is the k^{th} proper rotation component, and L_w^p is the trend component.

After the IWD transformation, the original input spectral curve X_w is decomposed into multiple proper rotation components (PRC_i) and a monotonic trend component (r). This method has the advantages of low computational complexity, high decomposition accuracy, robustness, and the effective avoidance of waveform superposition and modal aliasing.

F. HANKEL MATRIX

The Hankel matrix has many excellent properties, and as an excellent mathematical theory, it is widely used in numerical simulation calculations in various fields [37]. The elements on each inverse diagonal of the Hankel matrix were equal. In this study, PRCi, which better retains the original input spectral information after IWD processing, was selected to construct the Hankel matrix Z_a.

$$Z_a = \begin{bmatrix} x(1) & x(2) & \cdots & x(n) \\ x(2) & x(3) & \cdots & x(n+1) \\ \vdots & \vdots & \cdots & \vdots \\ x(m) & x(m+1) & \cdots & x(N) \end{bmatrix} \tag{6}$$

where $m \geq 2$, $n \geq 2$, and $1 < n < N$ and N is the number of sampling points in the original data. In $m = N - n + 1$, Z_a is a Hankel matrix.

G. SINGULAR VALUE DECOMPOSITION (SVD) AND SINGULAR ENTROPY (SE)

Singular value decomposition (SVD) means that any real matrix $A \in R^{m \times n}$ of any dimension can be decomposed into a product of three matrices, as shown in Equation (7).

$$A = USV^{\mathrm{T}} \tag{7}$$

where U is a unit orthogonal matrix, that is, its column vectors are unit vectors that are orthogonal to each other. V is the unit orthogonal matrix; that is, the row vectors are unit vectors that are orthogonal to each other, and are also the eigenvectors corresponding to the singular values. S is a diagonal matrix, $S = [diag(\sigma_1, \sigma_2, \sigma_3, \ldots, \sigma_m), O]$, where O represents a zero matrix and its diagonal matrix is a singular value [38].

Singular entropy (SE) is used to measure the amount of information of the signal component corresponding to the singular value, and the formula is as shown in Equations (8)–(9).

$$Y = -\sum_{i=1}^{n+1} E_i \ln E_i \tag{8}$$

$$E_i = \lambda_i / \sum_{i=1}^{n+1} \lambda_i \tag{9}$$

where E_i is the proportion of the i-th singular value and $\sum_{i=1}^{n+1} E_i = 1$, which satisfies the initial condition of the information entropy calculation.

The more complex the signal, the more useful the information, and the greater its singular entropy; in contrast, the smaller it is.

H. PARTIAL LEAST SQUARES REGRESSION (PLSR)

Partial least squares regression (PLSR) is a regression analysis method based on biased estimation. PLSR integrates multiple linear regression (MLR), canonical correlation analysis (CCA), and principal component analysis (PCA), which effectively overcomes the problem of multiple co-linearities among variables in modeling[28]. The principle is as follows:

There are p independent variables, $X = [x_1, x_2, \ldots, x_p]$; q dependent variables, $Y = [y_1, y_2, \ldots, y_q]$; and n sample observation points. Components t_1 and u_1 were extracted using PLSR in X and Y, respectively. Moreover, t_1 and u_1 should represent X and Y as much as possible, respectively, *and* t_1 and u_1 must have a high correlation. Establish the regression model of $y_1, y_2, \ldots, y_q$ to t_1; if the regression equation reaches a satisfactory accuracy, the algorithm stops. Otherwise, the second pair of principal components is extracted until satisfactory accuracy is achieved. The final expression is the regression equation between Y_1, $Y_2, \ldots, Y_{Q,}$ and the original variable, that is, the partial least squares regression equation.

I. ACCURACY EVALUATION OF THE MODEL

Pearson's correlation coefficient was used to analyze the correlation between the heavy metal content in maize leaves and different variables. The accuracy evaluation indicators of the model were the coefficient of determination (R^2) and root mean square error ($RMSE$). R^2 represents the correlation between predicted and measured values. If the correlation is higher, R^2 is closer to 1, indicating better prediction. $RMSE$ represents the deviation between the predicted and measured values. The smaller the $RMSE$ value, the smaller the variability of the prediction error, and the better the stability of the model [39].

$$R^2 = \frac{\sum_{i=1}^{n} (y_i - y_i')^2}{\sum_{i=1}^{n} (y_i - \bar{y})^2} \tag{10}$$

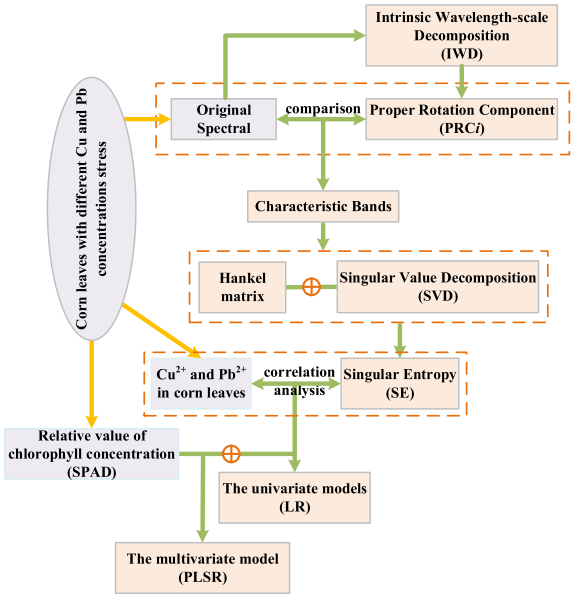

FIGURE 2. Overall technical flowchart for the research.

$$RMSE = \sqrt{\sum_{i=1}^{n} \frac{(y_i - y_i')^2}{n}} \tag{11}$$

where y_i and y_i' denote the measured and predicted values of the Cu and Pb content, respectively, $\bar{y}$ denotes the average measured value, and n represents the number of samples.

J. THE FRAMEWORK OF THE RESEARCH APPROACH

In this study, the steps for the inversion of Cu and Pb contents based on the IWD are as follows:

(1) IWD transformation was performed on the spectral data of leaves contaminated by heavy metals to obtain the PRC1, PRC2,…, and r components.

(2) PRC selection. Compare each PRCi component with the original input spectrum, and select the PRCi component that can better retain the original input spectrum information.

(3) Characteristic band selection. From the PRCi component, a band similar to the original input spectrum is selected as the characteristic band to construct the Hankel matrix and perform the SVD decomposition.

(4) Finally, singular entropy is obtained as the spectral information characteristic of heavy metal pollution. The correlation analysis between singular entropy and Cu and Pb content was carried out, the singular entropy with higher correlation was selected, a univariate model was established, and a multivariate model was established in conjunction with chlorophyll content to realize the prediction of Cu and Pb content. A research flowchart is shown in Figure 2.

III. RESULTS AND DISCUSSION

A. EFFECTS OF THE SPECTRAL REFLECTANCE OF MAIZE LEAVES UNDER CU AND PB STRESS

The average spectral curves of maize leaves under different Cu and Pb concentrations are shown in Figure 3. The spectral reflectance of leaves decreases with increasing Cu and

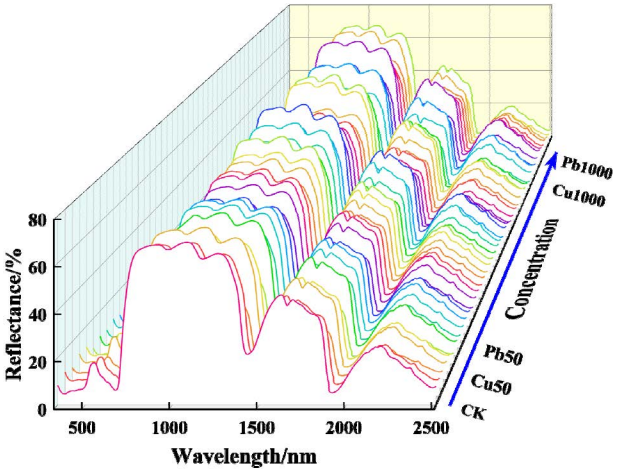

FIGURE 3. Spectral reflectance of corn leaves with different Cu and Pb concentrations stress (Note: The order of the spectral curves is sorted according to the spectral labels in Table 1).

Pb concentrations in the soil [40]. The 670-760 nm, where the reflectivity changes rapidly, is called the "red edge" of the plant in the electromagnetic spectrum [41]. In addition, some small weak peaks in the range–750-900 nm are mostly attributed to the third overtone stretch of O-H functional groups related to water in the corn leaf sample [42]. The absorption region in the range–900-980 nm, corresponds to the third overtone of the C-H functional groups (910 nm) and the second O-H overtone (960 nm) [43]. The spectral responses of maize leaves to different concentrations of Cu and Pb are too subtle [17]. Therefore, it is necessary to explore new spectral transformation methods to amplify stress information.

B. DETECTION OF COPPER, LEAD, AND CHLOROPHYLL CONTENT IN MAIZE LEAVES

The Cu^{2+} and Pb^{2+} contents and the relative values of chlorophyll in the maize leaves are shown in Figure 4(a-b). There were significant differences in the content of Cu^{2+} and Pb^{2+}, and the relative chlorophyll concentrations in maize leaves under different concentrations of Cu and Pb stress. It can be seen from Figure 4(a-b) that with the increase in Cu and Pb stress concentrations in the soil, the content of Cu^{2+} and Pb^{2+} in maize leaves also increased. This indicates that during maize growth, Cu^{2+} and Pb^{2+} enter the plant from the roots and are transported to the stems and leaves [44]. The accumulation and transfer of Cu and Pb in maize leaves directly or indirectly affects maize edibility. This study showed that heavy metals accumulate in the vegetation, which is consistent with previous studies [45]. Similarly, with an increase in Cu and Pb content in the soil, the relative value of chlorophyll content in maize leaves gradually decreased, indicating that the stress of heavy metals affected photosynthesis in maize plants, resulting in a decrease in chlorophyll content and a loss of green leaves [46]. Therefore, studying the Cu^{2+} and

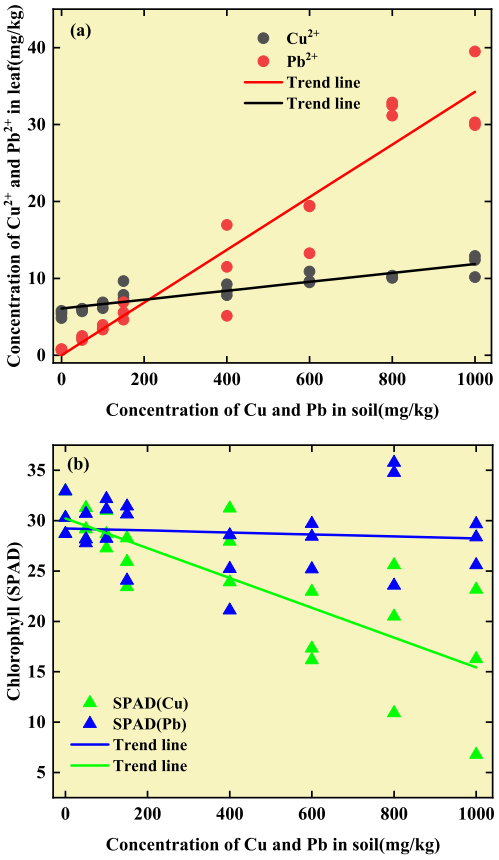

FIGURE 4. Detection value of Cu^{2+} and Pb^{2+} content and SPAD in corn leaves under different gradient stress.

Pb^{2+} contents in maize leaves is helpful for understanding the contamination of maize fruits.

C. IWD SPECTRAL TRANSFORMATION AND FEATURE BAND EXTRACTION

The IWD method was used to decompose the original spectrum of the leaves of the control group ck(0) to obtain two proper rotation components (PRC*i*) and one trend component (*r*), as shown in Figure 5. The IWD spectral transformation can effectively retain the original spectral information and avoid waveform superposition and modal aliasing. In comparison with the original spectrum, it was found that PRC1 and PRC2 fully retained the original spectrum information and amplified the reflectance of some bands in the original spectrum. Similarly, the IWD transformation of the spectra of corn leaves under different concentrations of Cu and Pb stress showed that the obtained PRC1 and PRC2 retained the original spectral information. Based on the spectral information retained by PRC1 and PRC2, A band similar to the original spectrum was selected as the characteristic band. The characteristic bands extracted from PRC1 are 553–680 nm, 681–780 nm, 1266–1429 nm, 1430–1631 nm, 1836–1913 nm, 1914–2111 nm. The characteristic bands extracted from PRC2 were 1263–1436, 1437–1627, 1820–1925, and 1926–2121 nm.

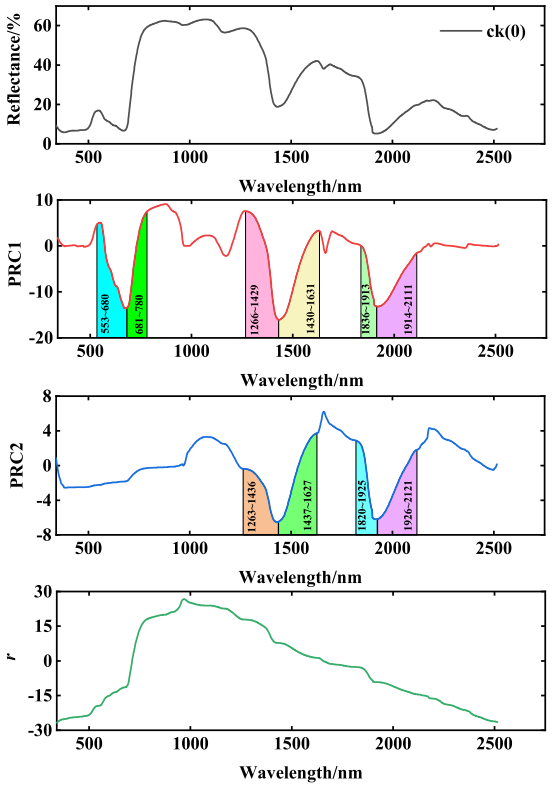

FIGURE 5. The results of IWD spectral transformation of corn leaves in ck(0) control group.

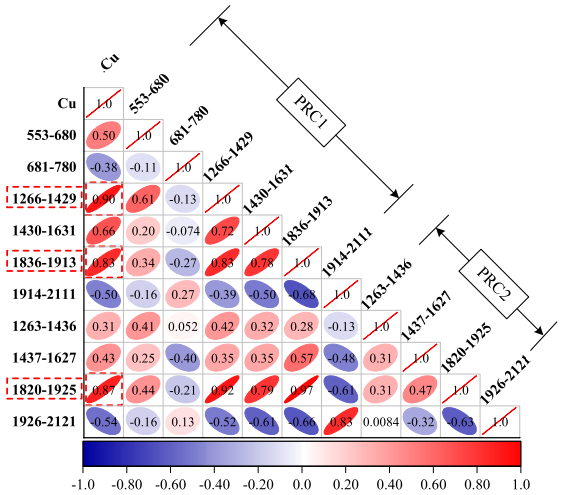

FIGURE 6. The correlation between the singular entropy of characteristic bands and the content of Cu^{2+} in corn leaves.

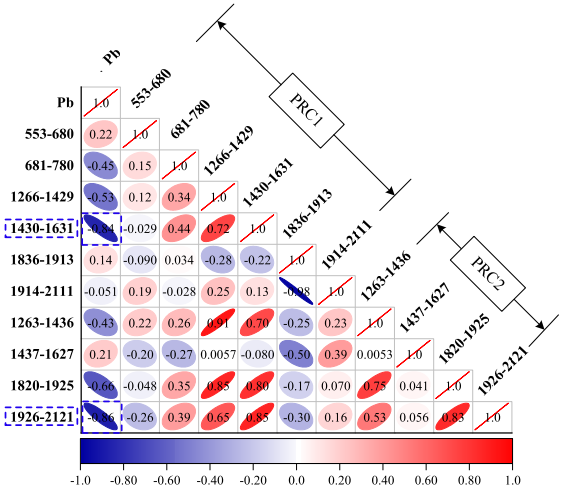

FIGURE 7. The correlation between the singular entropy of characteristic bands and the content of Pb^{2+} in corn leaves.

The Hankel matrix was constructed on the characteristic bands extracted by PRC1 and PRC2, the matrix was decomposed by SVD, and finally, singular entropy (SE) was obtained to analyze the monitoring effect. To further analyze the correlation between heavy metal content and spectral reflectance, Pearson correlation analysis was carried out between the SE corresponding to each characteristic band and the content of Cu^{2+} and Pb^{2+} in corn leaves, and the results are shown in Figure 6-7. The values in Figure 6-7 are the correlation coefficients; the direction of the ellipse to the right is a positive correlation, and the direction to the left is a negative correlation. They are extremely significant at a 0.01 level (both sides). All analyses were performed using SPSS Statistics 23.0, and all graphs were created using Origin software.

The singular entropies derived from the characteristic bands at 1266-1429 nm and 1836-1913 nm extracted by PRC1 and 1820-1925 nm extracted by PRC2 were strongly correlated with the Cu^{2+} content in maize leaves, with correlation coefficients as high as approximately 0.90. The singular entropy derived from the feature bands at 1430–1631 nm extracted by PRC1 and 1926–2121 nm extracted by PRC2 was strongly correlated with Pb^{2+} content in maize leaves, and the correlation coefficients were both as high as approximately 0.8. These optimal bands were observed in the near-infrared region. It can be seen that the two heavy metals are very sensitive to the near-infrared band, especially in the 1266-1913 nm and 1820-2121 nm. This finding suggests that these bands have the potential to predict the heavy metal content of vegetation. The correlation between the spectral variables transformed by the IWD and copper or lead content was significantly enhanced. The heavy metal Cu content had a significant positive correlation with the singular entropy of the optimal band, and the absolute value of r was 0.90. The lead content was negatively correlated with the singular entropy of the optimal band, and the absolute value of r was 0.86. This may be because the amount of spectral information in the leaves gradually decreased with the gradual increase in Pb content in the leaves. These variables may contain potential signatures owing to their statistically significant correlations. Therefore, we chose the band with the larger r as the optimal band, and the singular entropy corresponding to each optimal band was used as the input variable of the model.

D. CONSTRUCTION OF A UNIVARIATE MODEL

The singular entropy corresponding to the optimal band was selected to establish univariate models with Cu^{2+} and

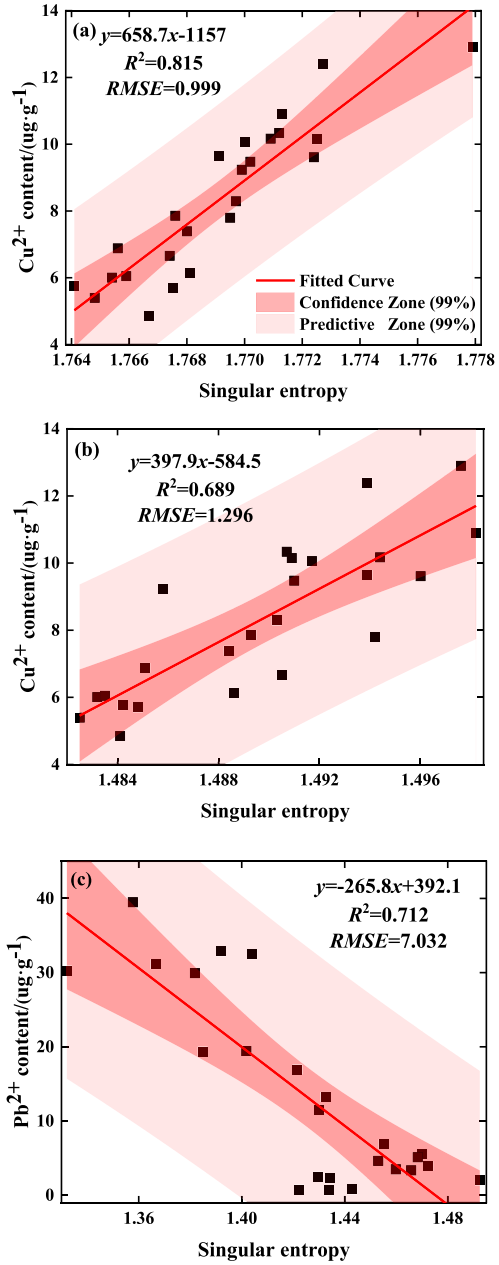

FIGURE 8. Models for estimating Cu^{2+} and Pb^{2+} content based on PRC1, (a) 1266-1429nm, (b) 1836-1913nm, (c) 1430-631nm.

Pb^{2+} contents in maize leaves. The scatter plot shows the results with the highest accuracy of the univariate model, and the results are shown in Figures 8-9. The singular entropy corresponding to the optimal bands of 1266–1429 nm and 1836–1913 nm extracted from PRC1 was strongly correlated with the Cu^{2+} content in maize leaves. The singular entropies corresponding to the best band at 1430–1631 nm extracted from PRC1 are strongly correlated with the Pb^{2+} content. The R^2 value of the prediction models was as high as 0.7, and the *RMSE* was 1.296. The singular entropy corresponding to the characteristic band of 1820–1925 nm extracted from PRC2 was strongly correlated with the Cu^{2+} content in maize leaves. The singular entropy corresponding to the

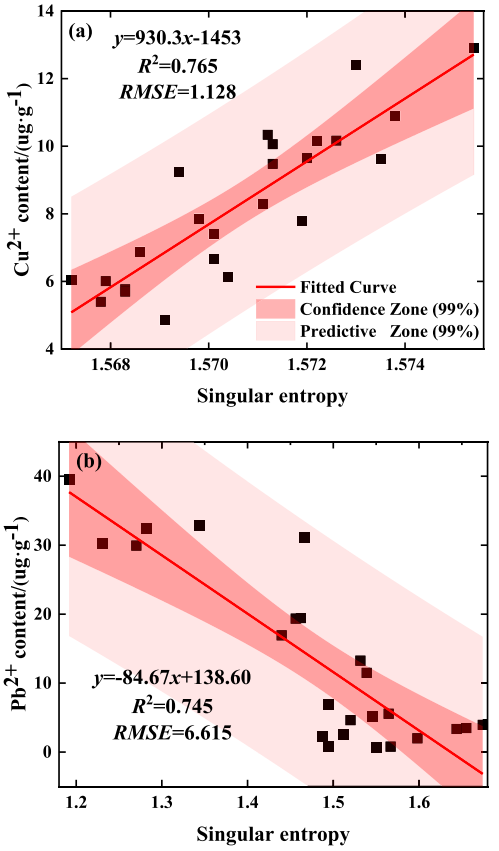

FIGURE 9. Models for estimating Cu^{2+} and Pb^{2+} content based on PRC2, (a) 1820-1925nm, (b) 1926-2121nm.

characteristic band 1926–2121 nm extracted by PRC2 was strongly correlated with the Pb^{2+} content. The R^2 value of the model was as high as approximately 0.76, and the *RMSE* was 1.128. Thus, these models show considerable promise for univariate modeling in predicting Cu and Pb contents in maize leaves and lay the foundation for the prediction of heavy metal content in vegetation. Therefore, compared with the univariate model, whether the multivariate model has better forecasting ability is worth further discussion.

E. CONSTRUCTION OF MULTIVARIATE MODELS

Changes in the chlorophyll content of plant leaves can also cause changes in visible and near-infrared spectral reflectance. With the increase in Cu and Pb stress concentrations, the Cu^{2+} and Pb^{2+} contents in the maize leaves increased gradually. Heavy metal stress has a negative effect on plant growth, causing changes in cell structure and water content, inhibiting photosynthesis, and reducing chlorophyll content [14], [47]. Finally, the relative value of chlorophyll concentration measured during data collection and the singular entropy (SE) calculated from the characteristic band were selected as parameters and combined with partial least square regression (PLSR) analysis to establish a multivariate model to predict the content of Cu^{2+} and Pb^{2+} in corn leaves. As shown in Figure 10, the predicted value of the multivariate model had a stronger correlation with the measured value,

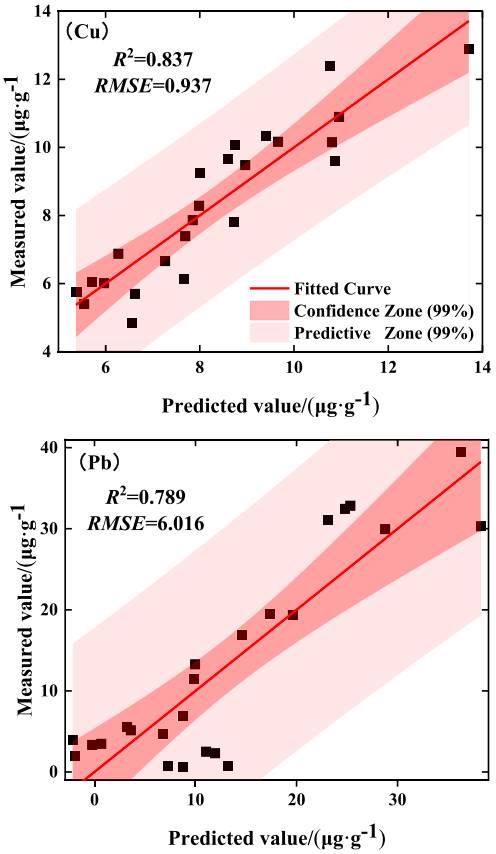

FIGURE 10. The multivariable models on predicting Cu^{2+} and Pb^{2+} content in corn leaves.

with an R^2 of approximately 0.8. Compared with univariate models, multivariate models are more robust and steadiest. This may be because the multivariate model integrates information from several different bands, which is consistent with previous studies [48].

Heavy metal pollution can cause changes in the chlorophyll content, cell structure, and water content of plants, thereby affecting the spectral reflectance of leaves. Nondestructive detection of Cu and Pb contents in crops can be achieved by monitoring subtle changes in spectral reflectance using hyperspectral techniques. This is consistent with previous studies showing that cell structure, spectral reflectance, and chlorophyll content can be used as parameters for the quantitative prediction of Cu and Pb content [49]. In this study, the optimal characteristic bands were determined by correlation analysis between the Cu^{2+} and Pb^{2+} content in maize leaves and spectral parameters. The results of this study show that spectral changes in the near-infrared band are significantly affected by the accumulation of Cu and Pb. Antonucci *et al.* also demonstrated that it is feasible to monitor heavy metal pollution using visible-light and near-infrared spectroscopy [50]. This study demonstrated that nonlinear models based on multivariate spectral bands are more accurate than linear models, which is consistent with previous results [51]. As shown in Figure 10, the multivariate model could better predict the Cu^{2+} and Pb^{2+} contents in maize leaves. The R^2 and *RMSE* values of the model are 0.837, 0.937, 0.789, and 6.016, respectively. This further confirms that the influence of Cu and Pb stress on leaf spectral reflectance is a complex process, and the high accuracy of the multivariate model can be attributed to the integration of multiple factors. The results of this study were satisfactory when compared with the discrete wavelet transform (DWT), traditional typical vegetation spectral parameters, and a variety of similar modeled spectral indices. Hyperspectral models are simple, inexpensive, and widely applicable. To further prove the reliability of this study, we verified the superiority and reproducibility of our proposed theoretical method.

F. VALIDATION OF THE SUPERIORITY OF THE MODELS

1) COMPARED WITH DISCRETE WAVELET TRANSFORM (DWT)

To verify the superiority of the model established based on the IWD transform in predicting heavy metal content in maize leaves, similar spectral transforms, such as the discrete wavelet transform (DWT), were selected to extract characteristic bands to establish models for comparative analysis. The main feature of wavelet analysis is the use of the expansion and translation of the wavelet function to characterize the local characteristics of the signal. The absorption and reflection spectra of the physicochemical components of vegetation have obvious local characteristics. Therefore, the use of wavelet analysis to transform vegetation spectral data can fully characterize the spectral information. The discrete wavelet transform can reduce redundant information and effectively extract the characteristic bands from spectral signals. Liu *et al.* showed that the db5 wavelet can accurately detect the singularity of crop spectra and effectively extract vegetation spectral information [52]. Here, the discrete wavelet transform (DWT) and db5 mother wavelet were used to decompose the leaf spectral curve into nine layers, the high-frequency coefficients of each layer were reconstructed, and correlation analysis was carried out with the content of Cu^{2+} and Pb^{2+} in the leaves. The results are shown in Figure 11(a-i). The wavelength with the largest correlation coefficient was selected as the optimal band, and a model was established to predict the Cu^{2+} and Pb^{2+} contents, as shown in Table 2. In terms of copper and lead content prediction, the model established by the wavelength selected after wavelet decomposition in the seventh layer could predict the Cu^{2+} and Pb^{2+} content in corn leaves well, but the maximum R^2 values were 0.769 and 0.693, respectively. These are not as good as the results obtained by the theoretical method proposed in this study, which confirms the superiority of the theoretical method proposed in this study.

2) COMPARED WITH TRADITIONAL TYPICAL VEGETATION SPECTRAL PARAMETERS

To verify the superiority of the model established by the IWD, traditional spectral characteristic parameters such as the maximum blue edge, maximum red shoulder, and height of the

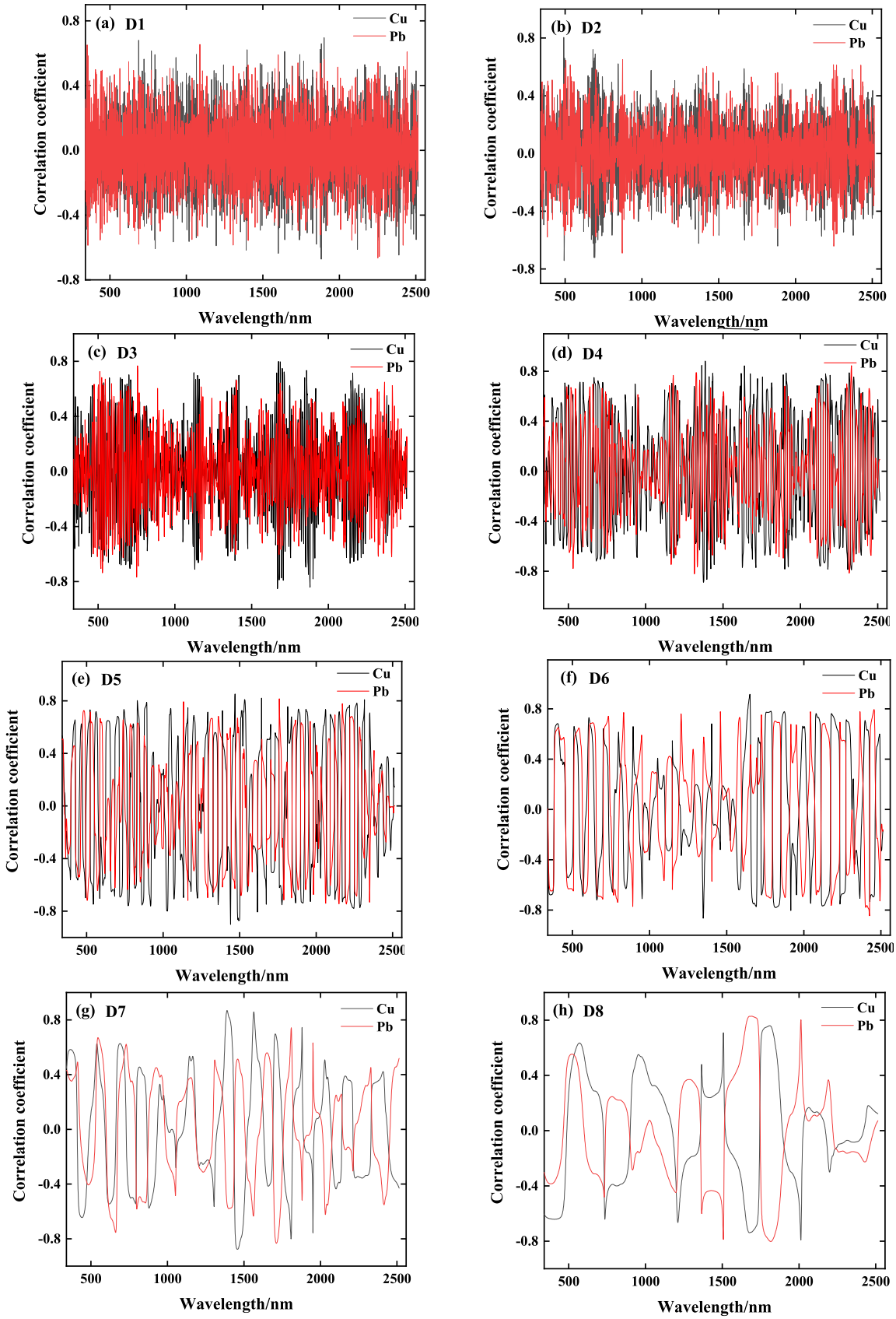

FIGURE 11. The correlation coefficient between the high-frequency coefficient of 9-layer wavelet decomposition and Cu^{2+}, Pb^{2+} content of leaves.

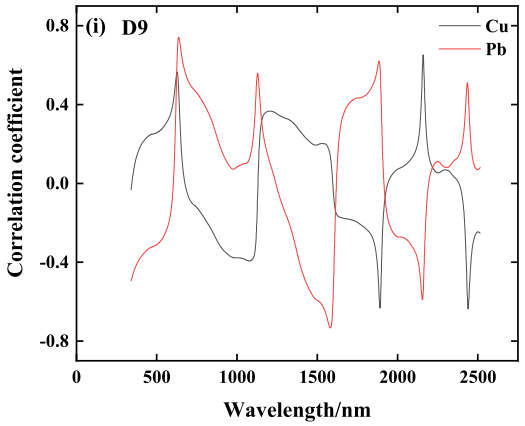

FIGURE 11. *(Continued.)* **The correlation coefficient between the high-frequency coefficient of 9-layer wavelet decomposition and Cu^{2+}, Pb^{2+} content of leaves.**

TABLE 2. **Model inversion results of wavelet transformation.**

Wavelet Coefficient Type	Heavy metal	Predictive expression	R^2	*RMSE*
D1	Cu	y= 402.92x + 0.058	0.484	1.672
	Pb	y = -2951.7x + 16.31	0.441	9.790
D2	Cu	y = 834.87x + 5.694	0.646	1.382
	Pb	y = -2598.7x + 15.845	0.475	9.482
D3	Cu	y = -534.39x + 7.495	0.725	1.219
	Pb	y = 3013.1x + 5.815	0.588	8.401
D4	Cu	y = 130.02x + 3.142	0.733	1.200
	Pb	y = 1034.5x + 15.921	0.683	7.372
D5	Cu	y = 150.88x + 3.422	0.724	1.220
	Pb	y = 1298.8x + 21.934	0.664	7.586
D6	Cu	y = -32.829x + 9.447	0.749	1.165
	Pb	y = 285.05x + 4.839	0.633	7.930
D7	Cu	y = -10.77x + 3.660	**0.769**	1.117
	Pb	y = -91.615x - 27.978	**0.693**	7.250
D8	Cu	y = -12.712x + 7.381	0.626	1.422
	Pb	y = 27.547x + 3.324	0.686	7.332
D9	Cu	y = 9.140x + 9.877	0.425	1.763
	Pb	y = 49.424x - 23.339	0.549	8.790

TABLE 3. **Name of spectral characteristic parameter.**

Parameter name	Definition
Blue edge maximum (BE)	The maximum value of the first derivative of the reflectance spectrum at 450~550nm
Red shoulder maximum (RS)	The maximum value of reflectance spectrum at 750~950nm
Green Peak Height (GH)	The maximum value of reflectance spectrum at 500~600nm

green peak were selected to establish models for comparative analysis, as shown in Figure 12 and Table 3 [53]. As shown in Table 4, in addition to the high accuracy of the green peak height in the Cu^{2+} content prediction, none of the Cu^{2+} and Pb^{2+} content prediction models using other spectral feature parameters achieved a high accuracy.

3) COMPARED TO THE NEW SPECTRAL INDEX

To verify the superiority of the theoretical approach proposed in this study further, we selected a variety of spectral indices

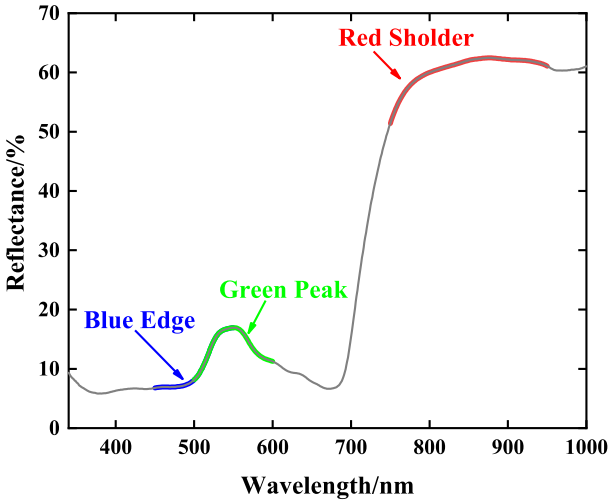

FIGURE 12. **The typical spectral reflectance of green vegetation and the main spectral features.**

TABLE 4. **Prediction of Cu^{2+} and Pb^{2+} content in corn leaves with spectral characteristic parameters.**

Parameter name	Heavy metal	Predictive expression	R^2	*RMSE*
BE	Cu	y=16.27x+2	0.23	2.03
	Pb	y=132.89x−34.89	0.45	9.65
RS	Cu	y = -0.035x + 10.38	0.01	2.31
	Pb	y = 0.526x−18.90	0.06	12.69
GH	Cu	y = 0.298x + 2.78	0.21	2.06
	Pb	y = 2.5406x−30.783	0.28	11.07

TABLE 5. **Spectral index for heavy metal content prediction in other studies.**

Spectral index	Formula/meaning	Reference
RVSI (Red dege vegetation stress index)	$(R_{712}+R_{752})/2-R_{732}$	[55]
LWVI (Leaf water vegetation index)	$(R_{1094}–R_{893})/(R_{1094}+R_{983})$	[56]
WBI (Water band index)	R_{900}/R_{970}	[57]
NDVIre (Red edge normalized difference vegetation index)	$(R_{750}-R_{705})/(R_{750}+R_{705})$	[58]
PSRI (Plant senescence frflectance index)	$(R_{678}-R_{500})/R_{750}$	[59]
YI (Yellowness index)	$-(R_{580}-2\times R_{624}+R_{668})/0.044^2$	[60]
CSVI (Copper stress vegetation index)	$(R_{550}\times R_{700})/(R_{850}\times R_{850})$	[61]
MSI (Moisture stress index)	R_{1600}/R_{820}	[62]
NDWI (Normalized difference water index)	$(R_{860}-R_{1240})/(R_{860}+R_{1240})$	[63]
DWSI (Disease water stress index)	$(R_{802}+R_{547})/(R_{1657}+R_{682})$	[56]

R_n: Reflections at a certain wavelength.

to build models for comparison. The model was established based on the relevant literature (Table 5). According to the spectral data obtained in our experiments, an expression

TABLE 6. Prediction of Cu^{2+} and Pb^{2+} content in corn leaves with spectral index.

Parameter name	Heavy metal	Predictive expression	R^2	*RMSE*
RVSI	Cu	$y = 1.761x + 11.595$	0.354	1.870
	Pb	$y = -8.6684x - 8.7438$	0.098	12.439
LWVI	Cu	$y = 262.54x + 6.368$	0.110	2.194
	Pb	$y = -1239.9x + 20.883$	0.150	12.074
WBI	Cu	$y = -149.26x + 161.65$	0.150	2.145
	Pb	$y = 902.5x - 915.3$	0.179	11.867
NDVIre	Cu	$y = -23.976x + 16.739$	0.496	1.651
	Pb	$y = -122.43x + 64.396$	0.164	11.972
PSRI	Cu	$y = -80.406x + 4.4072$	0.475	1.685
	Pb	$y = -458.67x - 3.501$	0.163	11.976
YI	Cu	$y = 0.002x + 7.768$	0.445	1.733
	Pb	$y = 0.005x + 14.246$	0.008	13.040
CSVI	Cu	$y = 30.368x + 5.008$	0.368	1.848
	Pb	$y = 264.21x - 6.9417$	0.162	11.989
MSI	Cu	$y = 49.725x - 26.163$	0.236	2.033
	Pb	$y = -248.78x + 181.32$	0.317	10.817
NDWI	Cu	$y = -197.5x + 13.487$	0.238	2.031
	Pb	$y = 443.13x + 1.309$	0.090	12.491
DWSI	Cu	$y = 7.155x - 3.936$	0.034	2.286
	Pb	$y = 81.315x - 126.78$	0.300	10.956

for the exponential model was obtained, and the Cu^{2+} and Pb^{2+} contents were predicted. Table 6 presents the results. As shown in Table 6, the PSRI and NDVIre spectral indices were strongly correlated with leaf Cu content, with R^2 values as high as 0.5. Previous studies have shown that the red edge is mainly determined by parameters such as the plant pigment and moisture [54]. They are highly sensitive to heavy metal contamination, and are often used to detect plant diseases and stress. RVSI also reflects subtle changes in the cell structure and chlorophyll content of crops under heavy metal stress [47]. However, in this study, PSRI and NDVIre were weakly correlated with Pb^{2+} content, which may be related to differences in the responses of specific vegetable varieties to Pb pollution. Other spectral indices, such as RVSI, LWVI, WBI, MSI, NDWI, and DWSI, cannot effectively predict Cu^{2+} and Pb^{2+} contents. Overall, the IWD proposed in this study is useful for enhancing the subtle differences in leaf spectra under Cu and Pb stress, amplifying the stress information, achieving Cu and Pb content predictions simultaneously, and with high reliability. This is of great significance for monitoring vegetation growth in heavy-metal-polluted environments in the future.

4) COMPARISON WITH OTHER SIMILAR STUDIES

To further demonstrate the advantages of this study, similar studies for estimating heavy metal content in plants were selected for comparison. Table 7 presents the results. As can be seen in Table 7, the results of this study can achieve better results when compared with other similar studies, regardless of whether it is the prediction of the copper or lead content. Simultaneously, the prediction accuracy of the multivariate PLSR model was higher than that of the conventional univariate model. Heavy metal stress in plants is affected by many other factors. Only a small number of studies were selected for comparative analysis. Whether this finding is generalizable requires further investigation in future studies.

TABLE 7. Comparisons of study results with other similar studies.

Method	Metals	R^2	Reference
GA	Pb	0.41	[64]
MLR	Cu	0.69	[65]
IWD+LR	Cu	0.69-0.81	This Work
IWD+LR	Pb	0.71-0.74	This Work
IWD+PLSR	Cu	0.837	This Work
IWD+PLSR	Pb	0.789	This Work

IV. CONCLUSION

In this study, hyperspectral data of maize leaves under different concentrations of Cu and Pb stress were obtained using an SVC HR-1024i spectrometer, and the Cu and Pb contents in the maize leaves were determined using an inductively coupled plasma optical emission spectrometer (ICP-OES). The changes of spectral characteristics of maize leaves caused by heavy metal copper and lead stress were difficult to identify the pollution degree according to the shape of the spectral curve. In this study, we proposed an innovative concept and method of IWD for preprocessing spectral data, extracting optimal feature bands, and inverting the Cu and Pb contamination information of maize leaves by constructing univariate and multivariate PLSR models to screen and predict the degree of Cu and Pb contamination in maize leaves.

The research results show that (1) PRC1 and PRC2 are obtained after the IWD transformation of spectral data, and bands similar to the original spectrum can be extracted as characteristic bands.

(2) The Hankel matrix was constructed for the characteristic band and singular entropy was obtained by SVD decomposition. The correlation between singular entropy and Cu and Pb contents was analyzed to obtain the optimal characteristic band for Cu and Pb content estimation.

(3) Univariate and multivariate PLSR models for Cu and Pb content prediction using the singular entropy corresponding to the optimal characteristic band. The R^2 value for the univariate model was approximately 0.7. The multivariate model had high accuracy, with an R^2 value of 0.8. Compared with the univariate model, the multivariate model exhibited stronger stability and robustness.

(4) The superiority of the theoretical method proposed in this study was further proven by comparing it with the discrete wavelet transform (DWT), typical vegetation spectral parameters, novel vegetation indices, and similar studies.

Studies have shown that reflectance spectroscopy can predict heavy metal content at large concentrations [66]. The optimal bands extracted in this study were all located in the near-infrared spectral region, which provides strong support for the in-depth exploration of near-infrared spectroscopy for monitoring heavy metal pollution. The IWD spectral

transformation proposed in this study will encourage more researchers to use the time-frequency analysis technique of the signal as a meaningful method to detect heavy metal pollution in vegetation. In this study, we only simulated the growth of maize plants under Cu and Pb stress through potted plants and predicted the heavy metal content in the leaves, which had certain limitations. Non-heavy metal stress (such as water stress and drought stress) is abrupt, and in future research, hyperspectral technology will be applied to the monitoring of vegetation growth under other types of heavy metals and non-heavy metal stress to further optimize and mine the universality and robustness of this method.

This study is of great significance and provides a reference for monitoring heavy metal pollution in vegetation. This experiment was carried out in a greenhouse, which has certain limitations. In future research, we will set up a heavy metal stress experiment in the field planting area, realize the monitoring of heavy metal pollution in large-scale vegetation through field experiments, and further verify the feasibility and generalizability of this research method.

REFERENCES

[1] Y. Wang, C. Tao, and B. Zou, "A transfer learning approach utilizing combined artificial samples for improved robustness of model to estimate heavy metal contamination in soil," *IEEE Access*, vol. 8, pp. 176960–176972, 2020.

[2] M. P. S. Khurana and P. Singh, "Waste water use in crop production: A review," *Resour. Environ.*, vol. 2, no. 4, pp. 116–131, Aug. 2012.

[3] E. Obeng-Gyasi, "Sources of lead exposure in various countries," *Rev. Environ. Health*, vol. 34, no. 1, pp. 25–34, Mar. 2019.

[4] B. Ma, R. Pu, S. Zhang, and L. Wu, "Spectral identification of stress types for maize seedlings under single and combined stresses," *IEEE Access*, vol. 6, pp. 13773–13782, 2018.

[5] G. Wang, Q. Wang, Z. Su, and J. Zhang, "Predicting copper contamination in wheat canopy during the full growth period using hyperspectral data," *Environ. Sci. Pollut. Res.*, vol. 27, pp. 39029–39040, Jul. 2020.

[6] X. Zhou, J. Sun, Y. Tian, K. Yao, and M. Xu, "Detection of heavy metal lead in lettuce leaves based on fluorescence hyperspectral technology combined with deep learning algorithm," *Spectrochim. Acta A, Mol. Biomol. Spectrosc.*, vol. 266, Feb. 2022, Art. no. 120460.

[7] E. Obeng-Gyasi, R. X. Armijos, M. M. Weigel, G. M. Filippelli, and M. A. Sayegh, "Cardiovascular-related outcomes in U.S. adults exposed to lead," *Int. J. Environ. Res. Public Health*, vol. 15, no. 4, Apr. 2018, Art. no. 759.

[8] P. Fu, W. Zhang, K. Yang, and F. Meng, "A novel spectral analysis method for distinguishing heavy metal stress of maize due to copper and lead: RDA and EMD-PSD," *Ecotoxicol. Environ. Saf.*, vol. 206, Dec. 2020, Art. no. 111211.

[9] K. Tan, H. Wang, L. Chen, Q. Du, P. Du, and C. Pan, "Estimation of the spatial distribution of heavy metal in agricultural soils using airborne hyperspectral imaging and random forest," *J. Hazardous Mater.*, vol. 382, Jan. 2020, Art. no. 120987.

[10] S. Zhang, J. Li, S. Wang, Y. Huang, Y. Li, Y. Chen, and T. Fei, "Rapid identification and prediction of cadmium-lead cross-stress of different stress levels in rice canopy based on visible and near-infrared spectroscopy," *Remote Sens.*, vol. 12, no. 3, Feb. 2020, Art. no. 469.

[11] C. Zhang, K. Yang, and W. Gao, "An experimental study on the influence of copper and lead concentration on the spectral reflectance of maize leaves," *Remote Sens. Lett.*, vol. 11, no. 12, pp. 1147–1156, Dec. 2020.

[12] C. Zhang, K. Yang, K. Rong, F. Cheng, and Y. Li, "The monitoring of the pollution degree of maize under copper stress," *J. Indian Soc. Remote Sens.*, vol. 48, no. 3, pp. 363–371, Mar. 2020.

[13] W. Zhang, P. Du, C. Lin, P. Fu, X. Wang, X. Bai, H. Zheng, J. Xia, and A. Samat, "An improved feature set for hyperspectral image classification: Harmonic analysis optimized by multiscale guided filter," *IEEE J. Sel. Topics Appl. Earth Observ. Remote Sens.*, vol. 13, pp. 3903–3916, 2020.

[14] T. Wang, H. Wei, C. Zhou, Y. Gu, R. Li, H. Chen, and W. Ma, "Estimating cadmium concentration in the edible part of capsicum annuum using hyperspectral models," *Environ. Monit. Assessment*, vol. 189, no. 11, Nov. 2017, Art. no. 548.

[15] G. Lassalle, S. Fabre, A. Credoz, D. Dubucq, and A. Elger, "Monitoring oil contamination in vegetated areas with optical remote sensing: A comprehensive review," *J. Hazardous Mater.*, vol. 393, Jul. 2020, Art. no. 122427.

[16] K. Yu, S. Fang, and Y. Zhao, "Heavy metal Hg stress detection in tobacco plant using hyperspectral sensing and data-driven machine learning methods," *Spectrochim. Acta A, Mol. Biomol. Spectrosc.*, vol. 245, Jan. 2021, Art. no. 118917.

[17] S. Jun, Z. Xin, W. Xiaohong, L. Bing, D. Chunxia, and S. Jifeng, "Research and analysis of cadmium residue in tomato leaves based on WT-LSSVR and vis-NIR hyperspectral imaging," *Spectrochim. Acta A, Mol. Biomol. Spectrosc.*, vol. 212, pp. 215–221, Apr. 2019.

[18] K. L. Smith, M. D. Steven, and J. J. Colls, "Use of hyperspectral derivative ratios in the red-edge region to identify plant stress responses to gas leaks," *Remote Sens. Environ.*, vol. 92, no. 2, pp. 207–217, Aug. 2004.

[19] Q. Shen, K. Xia, S. Zhang, C. Kong, Q. Hu, and S. Yang, "Hyperspectral indirect inversion of heavy-metal copper in reclaimed soil of iron ore area," *Spectrochim. Acta A, Mol. Biomol. Spectrosc.*, vol. 222, Nov. 2019, Art. no. 117191.

[20] K. Tan and P. Du, "Combined multi-kernel support vector machine and wavelet analysis for hyperspectral remote sensing image classification," *Chin. Opt. Lett.*, vol. 9, no. 1, Jan. 2011, Art. no. 011003.

[21] G. L. Sun, C. L. Zhang, Y. H. Fang, and H. H. Huang, "A method based on wavelet transform for spectral feature extraction," *Chin. J. Quantum Electron.*, 2006.

[22] X. Lin, Y.-C. Su, J. Shang, J. Sha, X. Li, Y.-Y. Sun, J. Ji, and B. Jin, "Geographically weighted regression effects on soil zinc content hyperspectral modeling by applying the fractional-order differential," *Remote Sens.*, vol. 11, no. 6, p. 636, Mar. 2019.

[23] X. Xu, M. Ren, J. Cao, Q. Wu, P. Liu, and J. Lv, "Spectroscopic diagnosis of zinc contaminated soils based on competitive adaptive reweighted sampling algorithm and an improved support vector machine," *Spectrosc. Lett.*, vol. 53, no. 2, pp. 86–99, Feb. 2020.

[24] J.-G. Xu, X.-L. Feng, L. Guan, S. Wang, and Q.-L. Hu, "Fractional differential application in reprocessing infrared spectral data," *Control Instrum. Chem. Ind.*, vol. 39, no. 3, pp. 347–351, 2012.

[25] C. Zhang, K. Yang, Y. Li, F. Cheng, and K. Rong, "Spectral characteristics and the study of pollution degree of maize leaves under copper and lead stress," *J. Indian Soc. Remote Sens.*, vol. 48, no. 1, pp. 21–33, Jan. 2020.

[26] P. H. Rathod, C. Brackhage, F. D. Van der Meer, I. Müller, M. F. Noomen, D. G. Rossiter, and G. E. Dudel, "Spectral changes in the leaves of barley plant due to phytoremediation of metals—Results from a pot study," *Eur. J. Remote Sens.*, vol. 48, no. 1, pp. 283–302, Jan. 2015.

[27] H.-Y. Ren, D.-F. Zhuang, J.-J. Pan, X.-Z. Shi, R.-H. Shi, and H.-J. Wang, "Study on canopy spectral characteristics of paddy polluted by heavy metals," *Spectrosc. Spectral Anal.*, vol. 30, no. 2, pp. 430–434, Feb. 2010.

[28] F. Wang, J. Gao, and Y. Zha, "Hyperspectral sensing of heavy metals in soil and vegetation: Feasibility and challenges," *ISPRS J. Photogramm. Remote Sens.*, vol. 136, pp. 73–84, Feb. 2018.

[29] Q. Tong, B. Zhang, and L. F. Zhang, "Current progress of hyperspectral remote sensing in China," *J. Remote Sens.*, vol. 20, no. 5, pp. 689–707 2016.

[30] Y. Zhang, L. Zhang, X. Bai, and L. Zhang, "Infrared and visual image fusion through infrared feature extraction and visual information preservation," *Infr. Phys. Technol.*, vol. 83, pp. 227–237, Jun. 2017.

[31] Y. Hong, R. Shen, H. Cheng, S. Chen, Y. Chen, L. Guo, J. He, Y. Liu, L. Yu, and Y. Liu, "Cadmium concentration estimation in peri-urban agricultural soils: Using reflectance spectroscopy, soil auxiliary information, or a combination of both?" *Geoderma*, vol. 354, Nov. 2019, Art. no. 113875.

[32] P. Fu, K. Yang, F. Meng, W. Zhang, Y. Cui, F. Feng, and G. Yao, "A new three-band spectral and metal element index for estimating soil arsenic content around the mining area," *Process Saf. Environ. Protection*, vol. 157, pp. 27–36, Jan. 2022.

[33] M. Wang, K.-M. Yang, and W. Zhang, "Hyperspectral monitoring of maize leaves under copper stress at different growth stages," *Remote Sens. Lett.*, vol. 11, no. 4, pp. 343–352, Apr. 2020.

[34] J. Ma, S. Han, C. Li, L. Zhan, and G. Zhang, "A new method based on time-varying filtering intrinsic time-scale decomposition and general refined composite multiscale sample entropy for rolling-bearing feature extraction," *Entropy*, vol. 23, no. 4, Apr. 2021, Art. no. 451.

[35] M. G. Frei and I. Osorio, "Intrinsic time-scale decomposition: Time–frequency–energy analysis and real-time filtering of non-stationary signals," *Proc. Roy. Soc. A, Math., Phys. Eng. Sci.*, vol. 463, no. 2078, pp. 321–342, Feb. 2007.
[36] A. Hu, X. Yan, and L. Xiang, "A new wind turbine fault diagnosis method based on ensemble intrinsic time-scale decomposition and WPT-fractal dimension," *Renew. Energy*, vol. 83, pp. 767–778, Nov. 2015.
[37] S. Al-Homidan, "Hankel matrix transforms and operators," *J. Inequal. Appl.*, vol. 2012, no. 1, pp. 1–9, Dec. 2012.
[38] Z. Su, Y. Zhang, M. Jia, F. Xu, and J. Hu, "Gear fault identification and classification of singular value decomposition based on Hilbert–Huang transform," *J. Mech. Sci. Technol.*, vol. 25, no. 2, pp. 267–272, Feb. 2011.
[39] L. He, X. Song, W. Feng, B.-B. Guo, Y.-S. Zhang, Y.-H. Wang, C.-Y. Wang, and T.-C. Guo, "Improved remote sensing of leaf nitrogen concentration in winter wheat using multi-angular hyperspectral data," *Remote Sens. Environ.*, vol. 174, pp. 122–133, Mar. 2016.
[40] Y. W. Gu, S. Li, W. Gao, and H. Wei, "Hyperspectral estimation of the cadmium content in leaves of *Brassica rapa* Chinesis based on the spectral parameters," *Acta Ecol. Sinica*, vol. 35, no. 13, pp. 4445–4453, 2015.
[41] A. Reinart and T. Kutser, "Comparison of different satellite sensors in detecting cyanobacterial Bloom events in the Baltic sea," *Remote Sens. Environ.*, vol. 102, nos. 1–2, pp. 74–85, May 2006.
[42] U. Khulal, J. Zhao, W. Hu, and Q. Chen, "Nondestructive quantifying total volatile basic nitrogen (TVB-N) content in chicken using hyperspectral imaging (HSI) technique combined with different data dimension reduction algorithms," *Food Chem.*, vol. 197, pp. 1191–1199, Apr. 2016.
[43] W. Camacho, A. Vallés-Lluch, A. Ribes-Greus, and S. Karlsson, "Determination of moisture content in nylon 6,6 by near-infrared spectroscopy and chemometrics," *J. Appl. Polym. Sci.*, vol. 87, no. 13, pp. 2165–2170, Mar. 2003.
[44] T. Yoneyama, T. Gosho, M. Kato, S. Goto, and H. Hayashi, "Xylem and phloem transport of Cd, Zn and Fe into the grains of rice plants (*Oryza sativa* L.) grown in continuously flooded Cd-contaminated soil," *Soil Sci. Plant Nutrition*, vol. 56, no. 3, pp. 445–453, Jun. 2010.
[45] L. Hernández-Bautista, L. I. Trejo-Téllez, F. C. Gomez-Merino, S. Garcia-Morales, and O. Tejeda-Sartorius, "Physiological and nutrient changes in sweet pepper (*Capsicum annuum* L.) seedlings caused by cadmium," *Revista Internacional De Contaminacion Ambiental*, vol. 31, no. 4, pp. 389–396, 2015.
[46] M. Ovečka and T. Takáč, "Managing heavy metal toxicity stress in plants: Biological and biotechnological tools," *Biotechnol. Adv.*, vol. 32, no. 1, pp. 73–86, Jan. 2014.
[47] L. Guan, "Hyperspectral recognition models for physiological ecology characterization of rice in Cd pollution stress," *Ecol. Environ. Sci.*, 2009.
[48] T. Shi, Y. Chen, Y. Liu, and G. Wu, "Visible and near-infrared reflectance spectroscopy—An alternative for monitoring soil contamination by heavy metals," *J. Hazardous Mater.*, vol. 265, pp. 166–176, Jan. 2014.
[49] L. Guan and X. Liu, "Experimental research on remote sensing diagnosis method of Cd pollution stress in rice," *Trans. CSAE*, vol. 25, no. 6, pp. 168–173, 2009.
[50] F. Antonucci, P. Menesatti, N. M. Holden, E. Canali, S. Giorgi, A. Maienza, and S. R. Stazi, "Hyperspectral visible and near-infrared determination of copper concentration in agricultural polluted soils," *Commun. Soil Sci. Plant Anal.*, vol. 43, no. 10, pp. 1401–1411, May 2012.
[51] Y. H. Zhang, W. H. Chen, Q. Y. Guo, and Q. Zhang, "Hyperspectral estimation models for photosynthetic pigment contents in leaves of Eucalyptus," *Acta Ecol. Sinica*, vol. 33, no. 3, pp. 876–887, 2013.
[52] M. Liu, X. Liu, L. Wu, L. Duan, and B. Zhong, "Wavelet-based detection of crop zinc stress assessment using hyperspectral reflectance," *Comput. Geosci.*, vol. 37, no. 9, pp. 1254–1263, Sep. 2011.
[53] C. Zhang, H. Ren, X. Dai, Q. Qin, J. Li, T. Zhang, and Y. Sun, "Spectral characteristics of copper-stressed vegetation leaves and further understanding of the copper stress vegetation index," *Int. J. Remote Sens.*, vol. 40, no. 12, pp. 4473–4488, Jun. 2019.
[54] M. Liu, X. Liu, W. Ding, and L. Wu, "Monitoring stress levels on rice with heavy metal pollution from hyperspectral reflectance data using wavelet-fractal analysis," *Int. J. Appl. Earth Observ. Geoinf.*, vol. 13, no. 2, pp. 246–255, Apr. 2011.
[55] R. Merton and J. Huntington, "Early simulation results of the ARIES-1 satellite sensor for multi-temporal vegetation research derived from AVIRIS," Tech. Rep., 1999.
[56] L. S. Galvão, A. R. Formaggio, and D. A. Tisot, "Discrimination of sugarcane varieties in southeastern Brazil with EO-1 hyperion data," *Remote Sens. Environ.*, vol. 94, no. 4, pp. 523–534, Feb. 2005.
[57] J. Penuelas, J. Pinol, R. Ogaya, and I. Filella, "Estimation of plant water concentration by the reflectance water index WI (R900/R970)," *Int. J. Remote Sens.*, vol. 18, no. 13, pp. 2869–2875, Sep. 1997.
[58] A. Gitelson and M. N. Merzlyak, "Spectral reflectance changes associated with autumn senescence of *Aesculus hippocastanum* L. and *Acer platanoides* L. leaves. Spectral features and relation to chlorophyll estimation," *J. Plant Physiol.*, vol. 143, no. 3, pp. 286–292, Mar. 1994.
[59] M. N. Merzlyak, A. A. Gitelson, O. B. Chivkunova, and V. Y. Rakitin, "Non-destructive optical detection of pigment changes during leaf senescence and fruit ripening," *Physiol. Plantarum*, vol. 106, no. 1, pp. 135–141, May 1999.
[60] M. L. Adams, W. D. Philpot, and W. A. Norvell, "Yellowness index: An application of spectral second derivatives to estimate chlorosis of leaves in stressed vegetation," *Int. J. Remote Sens.*, vol. 20, no. 18, pp. 3663–3675, Jan. 1999.
[61] C. Zhang, H. Ren, Q. Qin, and O. K. Ersoy, "A new narrow band vegetation index for characterizing the degree of vegetation stress due to copper: The copper stress vegetation index (CSVI)," *Remote Sens. Lett.*, vol. 8, no. 6, pp. 576–585, Jun. 2017.
[62] B. N. Rock, J. E. Vogelmann, D. L. Williams, A. F. Vogelmann, and T. Hoshizaki, "Remote detection of forest damage," *BioScience*, vol. 36, no. 7, pp. 439–445, Aug. 1986.
[63] B.-C. Gao, "NDWI—A normalized difference water index for remote sensing of vegetation liquid water from space," *Remote Sens. Environ.*, vol. 58, no. 3, pp. 257–266, Dec. 1996.
[64] Q. Jiang, M. Liu, J. Wang, and F. Liu, "Feasibility of using visible and near-infrared reflectance spectroscopy to monitor heavy metal contaminants in urban lake sediment," *Catena*, vol. 162, pp. 72–79, Mar. 2018.
[65] P. Wang, X.-N. Liu, and F. Huang, "Retrieval model for subtle variation of contamination stressed maize chlorophyll using hyperspectral data," *Spectrosc. Spectral Anal.*, vol. 30, no. 1, pp. 197–201, Jan. 2010.
[66] C. M. Pandit, G. M. Filippelli, and L. Li, "Estimation of heavy-metal contamination in soil using reflectance spectroscopy and partial least-squares regression," *Int. J. Remote Sens.*, vol. 31, no. 15, pp. 4111–4123, 2010.

JIANHONG ZHANG (Student Member, IEEE) received the M.S. degree in mining engineering from the Inner Mongolia University of Science and Technology, China, in 2016. She is currently pursuing the Ph.D. degree in photogrammetry and remote sensing with the School of Earth Sciences and Surveying Engineering, China University of Mining and Technology-Beijing, China. Her research interests include heavy metal pollution monitoring with hyperspectral remote sensing, and remote sensing monitoring technology for environmental and geological disasters.

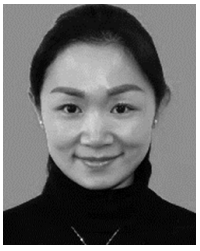

MIN WANG received the Ph.D. degree in photogrammetry and remote sensing from the School of Earth Sciences and Surveying Engineering, China University of Mining and Technology-Beijing, China. Her research interests include heavy metal pollution monitoring with hyperspectral remote sensing, and remote sensing monitoring technology for environmental and geological disasters.

KEMING YANG received the Ph.D. degree in photogrammetry and remote sensing from the China University of Mining and Technology-Beijing, Beijing, China, in 2007. He is currently a Professor with the College of Geoscience and Surveying Engineering, China University of Mining and Technology-Beijing. His research interests include hyperspectral remote sensing, remote sensing of land resources and environment, and deformation/environmental monitoring and prevention.

BING WU received the M.S. degree in surveying and mapping engineering from the North China University of Science and Technology, China, in 2020. He is currently pursuing the Ph.D. degree in photogrammetry and remote sensing with the School of Earth Sciences and Surveying Engineering, China University of Mining and Technology-Beijing, China. His research interests include heavy metal pollution monitoring with hyperspectral remote sensing, and remote sensing monitoring technology for environmental and geological disasters.

YAXING LI is currently with the School of Earth Science and Mapping Engineering, China University of Mining and Technology-Beijing. His research interest includes InSAR combined with mining subsidence.

YANRU LI received the B.E. degree in surveying and mapping engineering from the Shandong University of Science and Technology, in 2019. She is currently pursuing the Ph.D. degree in science and technology of surveying and mapping with the School of Earth Sciences and Surveying Engineering, China University of Mining and Technology-Beijing, China. Her research interests include heavy metal pollution monitoring with hyperspectral remote sensing, and remote sensing monitoring technology for environmental and geological disasters.

QIANQIAN HAN received the bachelor's degree in surveying and mapping engineering from Inner Mongolia Agricultural University, in 2019. She is currently pursuing the master's degree in photogrammetry and remote sensing with the School of Earth Science and Surveying and Mapping Engineering, China University of Mining and Technology-Beijing. Her research interests include heavy metal pollution monitoring with hyperspectral remote sensing, and remote sensing monitoring technology for environmental and geological disasters.